Journal of Power Sources 230 (2013) 138–142

Contents lists available at SciVerse ScienceDirect

Journal of Power Sources

journal homepage: www.elsevier.com/locate/jpowsour

Short communication

Structurally stabilized $LiNi_{0.5}Mn_{1.5}O_4$ with enhanced electrochemical properties through nitric acid treatment

Jun Soo Park [a,b], Kwang Chul Roh [a,*], Jae-Won Lee [c], Kyeongse Song [d], Yong-Il Kim [e], Yong-Mook Kang [d,**]

[a] KICET, 233-5 Gasan-dong, Guemcheon-Gu, Seoul 153-801, Republic of Korea
[b] Department of WCU Energy Engineering, Hanyang University, 17 Haengdang-dong, Seongdong-gu, Seoul 133-791, Republic of Korea
[c] Department of Energy Engineering, Dankook University, Cheonan 330-714, Republic of Korea
[d] Department of Chemistry, Dongguk University-Seoul, 100715 Seoul, Republic of Korea
[e] Korea Research Institute of Standards and Science (KRISS), Daejeon 305-340, Republic of Korea

HIGHLIGHTS

- $LiNi_{0.5}Mn_{1.5}O_4$ is treated with nitric acid to reduce the degree of cation ordering.
- The loss of cation ordering makes $LiNi_{0.5}Mn_{1.5}O_4$ *Fd3m*-like.
- This structural change significantly enhances its electrochemical properties.

GRAPHICAL ABSTRACT

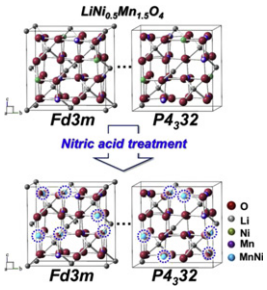

ARTICLE INFO

Article history:
Received 1 November 2012
Received in revised form
8 December 2012
Accepted 11 December 2012
Available online 20 December 2012

Keywords:
Lithium rechargeable battery
Cathode
Spinel structure
Nitric acid treatment
Cation ordering

ABSTRACT

We demonstrate the effects of reduced cation ordering on the electrochemical properties of $LiNi_{0.5}Mn_{1.5}O_4$. $LiNi_{0.5}Mn_{1.5}O_4$ is treated with nitric acid to reduce the degree of cation ordering. Nitric acid treatment induces partial oxidation of Ni^{2+} to Ni^{3+} as confirmed by X-ray photoelectron spectroscopy (XPS). Thanks to this oxidation, the 16d octahedral site in $LiNi_{0.5}Mn_{1.5}O_4$ is quite void of cation ordering and its structure is partially changed to more disordered spinel engaged in *Fd3m*. This structural change is accompanied by significantly enhanced electrochemical performances in rate capability as well as cyclic retention. Actually, nitric acid treated $LiNi_{0.5}Mn_{1.5}O_4$ can deliver about 87% of the initial capacity (129 mAh g^{-1}) even after 100 cycles even at 55 °C.

1. Introduction

High-energy and high-power rechargeable Li-ion batteries are the essential components of portable electronic devices and hybrid-electric vehicles [1]. $LiMn_2O_4$ spinels have been extensively investigated due to their low cost, easy preparation, safety, and environmental advantages [2,3]. However, this material suffers from poor cycling behavior especially at high temperature [4]. Although the origin of this capacity fading has not been fully understood, several possible mechanisms have been suggested, including the Jahn–Teller distortion, the dissolution of Mn at high temperature originating from the $Mn^{3+/4+}$ redox, and the change in the crystal lattice arrangement with cycling [5–9].

* Corresponding author. Tel.: +82 17 544 2733; fax: +82 23 282 2475.
** Corresponding author. Tel.: +82 10 3257 9051.
E-mail addresses: rkc@kicet.re.kr (K.C. Roh), dake1234@dongguk.edu, dake@kaist.ac.kr (Y.-M. Kang).

0378-7753/$ – see front matter © 2012 Elsevier B.V. All rights reserved.
http://dx.doi.org/10.1016/j.jpowsour.2012.12.051

As one of the ways to improve the poor cycling behavior of $LiMn_2O_4$, metal substitution into its framework has been suggested resultantly introducing the transition metal-substituted spinel materials ($LiM_xMn_{2-x}O_4$, M = Cr, Ni, Co, Fe, Cu, Al, etc.) with higher voltage plateau around 5 V [10–13]. The capacity and potential plateau of $LiM_xMn_{2-x}O_4$ are tentatively dependent on the kind of transition metals used and their content. Among them, $LiNi_{0.5}Mn_{1.5}O_4$ has drawn the greatest attention for its advantageous plateau evolution that two potential plateaus are commonly developed around 4.7 V differing from other spinel materials with two separate plateaus at 4.0 and 5 V [12]. The characteristic potential plateaus of $LiNi_{0.5}Mn_{1.5}O_4$ around 4.7 V are each attributed to the redox reactions of Ni^{2+}/Ni^{3+} and Ni^{3+}/Ni^{4+}. Even if $LiNi_{0.5}Mn_{1.5}O_4$ exhibits high discharge capacity with quite stable cyclic retention, the reaction between its surface and electrolyte at high operating voltage as well as the ordering of Ni^{2+} and Mn^{4+} ions in the 16d octahedral sites of the spinel lattice results in an inevitable capacity fading particularly at elevated temperatures and a poor rate capability, which preventing its commercialization [10–14].

Previous reports indicate that $LiNi_{0.5}Mn_{1.5}O_4$ has two different crystal structures engaged in *P4₃32* (stoichiometric ordered $LiNi_{0.5}Mn_{1.5}O_4$) in which Mn ions are only composed of Mn^{4+}; and *Fd3m* (non-stoichiometric disordered $LiNi_{0.5}Mn_{1.5}O_{4-\delta}$) where the oxidation state of Mn ions can be diversified from Mn^{3+} to Mn^{4+}. Non-stoichiometric $LiNi_{0.5}Mn_{1.5}O_{4-\delta}$ has face-centered cubic spinel structure (*Fd3m*) where Ni and Mn atoms are randomly distributed in 16d sites while Li and O occupy 8a tetrahedral sites and 32e sites, respectively [15,16]. On the other hand, stoichiometric $LiNi_{0.5}Mn_{1.5}O_4$ has a primitive simple cubic structure (*P4₃32*) in which Ni, Mn and Li atoms occupy totally different sites each corresponding 4a, 12d, 4c, whereas O atoms resides in 8c and 24e sites. It has been well known that non-stoichiometric $LiNi_{0.5}Mn_{1.5}O_{4-\delta}$ with the disordered distribution of Ni and Mn in 16d site exhibits superior electrochemical performances to stoichiometric one [17].

In this paper, we suggest the effect of nitric acid treatment on the structure and electrochemical properties of $LiNi_{0.5}Mn_{1.5}O_4$. Various structural analyses including XPS, XRD, Raman spectroscopy prove that nitric acid treatment induces the disordering of Ni and Mn especially on the surface of $LiNi_{0.5}Mn_{1.5}O_4$ resultantly rendering the structure of as-synthesized $LiNi_{0.5}Mn_{1.5}O_4$ more *Fd3m*-like. The electrochemical analyses inform that the surface-treated $LiNi_{0.5}Mn_{1.5}O_4$ using nitric acid is almost void of the redox trace of Ni^{2+}/Ni^{3+} during reduction clearly due to the partial oxidation of Ni^{2+} to Ni^{3+} as confirmed by X-ray photoelectron spectroscopy. This means that Mn^{4+} is reduced to Mn^{3+} for the charge balance clearly proving that the surface structure of as-synthesized $LiNi_{0.5}Mn_{1.5}O_4$ becomes more *Fd3m*-like. Herein, the structure and the electrochemical properties of the surface-treated $LiNi_{0.5}Mn_{1.5}O_4$ will be discussed in comparison with the bare one.

2. Experimental

2.1. Preparation of $LiNi_{0.5}Mn_{1.5}O_4$

$LiNi_{0.5}Mn_{1.5}O_4$ spinels were prepared by the carbon combustion method. The stoichiometric amounts of lithium nitrate ($LiNO_3$, 5% excess), nickel nitrate ($Ni(NO_3)_2 \cdot 6H_2O$) and manganese nitrate ($Mn(NO_3)_2 \cdot 6H_2O$) were dissolved in distilled water to obtain a 1 M solution. 1 mol of sucrose was dissolved in the nitrates solution and then the solution was heated at 80 °C for 3 h. The temperature of the solution was increased to 120 °C. After a few minutes, the mass starts to burn up spontaneously without flame. The product of the reaction ("as-prepared") sample was ground into a powder. Then the as-prepared samples were heated at 800 °C for 4 h and subsequently annealed at 600 °C for 10 h. The obtained powder was immersed in an aqueous HNO_3 solution (1 M) for 15 h at room temperature to oxidize the surface, then dried and annealed in N_2 gas atmosphere at 400 °C for 1 h.

2.2. Electrochemical experiment

The electrodes were prepared by pasting an aqueous slurry containing 80 wt.% obtained powder, 10 wt.% Super-P, and 10 wt.% polyvinylidene fluoride (PVDF). The electrodes were then dried at 120 °C for 24 h under vacuum. The cast electrodes were cut to a size of φ12. The final loading density of the electrode material (i.e., the annealed $LiNi_{0.5}Mn_{1.5}O_4$ powder) was 5.5 mg cm^{-2}. The electrolyte was 1.15 M $LiPF_6$ in a mixture of ethyl carbonate (EC), ethyl-methyl carbonate (EMC) and dimethyl carbonate (DMC) (PANAX, South Korea). 2032 coin-type half-cells were fabricated using metallic lithium foil as a counter electrode.

2.3. Structure characterization

The phase components of the samples were investigated by powder X-ray diffractometry (XRD, Rigaku, D/Max-2500) with Cu K radiation. In order to exactly figure out the real structure and symmetry before and after nitric acid treatment, Rietveld refinement was carried out on pristine- and surface-treated-$LiNi_{0.5}Mn_{1.5}O_4$. The $Fd\bar{3}m$ initial crystal structural model of two samples were constructed with crystallographic data based on $Fd\bar{3}m$ and *P4₃32*. The morphology of these samples was examined using field scanning electron microscopy (FE-SEM, JEOL, JSM-7000F). The Raman spectra for pristine- and surface-treated-$LiNi_{0.5}Mn_{1.5}O_4$ were also collected with a Confocal Laser Micro Raman Spectrometer (LABRAM-HR, Jobin Yvon) using an excitation light of 514.5 nm from Ar ion laser. X-ray photoelectron spectroscopy (XPS) was performed to determine the average oxidation of states Ni and Mn in the materials. XPS spectra were collected on PHI 5000 VersaProbe™ equipment (ULVAC-PHI) with a non-monochromatic Al Kα _ (1486.6 eV) light source. The cyclic voltammograms of the cells were characterized using a potentiostat (VSP, Biologic). The capabilities and cycle performances of the half-cell were tested on a battery tester (Maccor, S-4000).

3. Results and discussion

XRD patterns of pristine $LiNi_{0.5}Mn_{1.5}O_4$ and surface-treated one using nitric acid are presented in Fig. 1. It is obvious that all of reflections are similar to the conventional $LiNi_{0.5}Mn_{1.5}O_4$ with spinel structure. However, because the peaks coming from pristine $LiNi_{0.5}Mn_{1.5}O_4$ and surface-treated one could not be discriminated without any detailed refinement, we conducted Rietveld refinement to identify their structures. A careful examination revealed that even if the two XRD patterns are somewhat different, they fundamentally seem to be engaged in the same space group (*Fd3m*). Comparative refinements for the XRD patterns of pristine sample and surface-treated one suggest that two reflections can be indexed to *P4₃32* or *Fd3m*. (Fig. S1 and S2) This result indicates that the bulk structure of $LiNi_{0.5}Mn_{1.5}O_4$ is constructed in the mixed framework composed of *P4₃32* or *Fd3m*, and maintains its original symmetry and structure irrespective of nitric acid treatment. Hence, it is evident that the effect of nitric acid treatment is confined to the surface structure of $LiNi_{0.5}Mn_{1.5}O_4$ [11]. More detailed structural change after nitric acid treatment has been exploited by X-ray photoelectron spectroscopy (XPS) and Raman spectroscopy.

XPS was conducted to figure out the surface structure of $LiNi_{0.5}Mn_{1.5}O_4$ before or after nitric acid treatment. The binding energy change offers the information mainly on the oxidation state

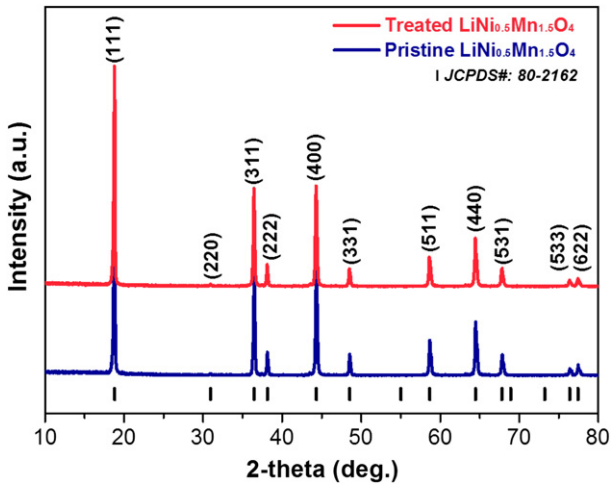

Fig. 1. X-ray diffraction patterns of the pristine $LiNi_{0.5}Mn_{1.5}O_4$ and surface-treated $LiNi_{0.5}Mn_{1.5}O_4$ samples.

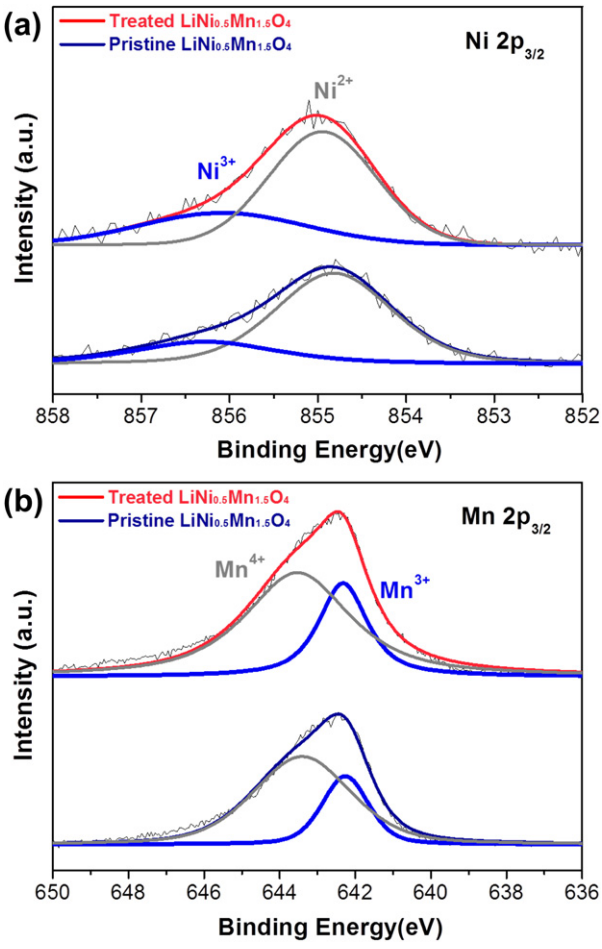

Fig. 2. X-ray photoelectron spectra of the pristine and surface-treated $LiNi_{0.5}Mn_{1.5}O_4$ samples: (a) the Ni $2p_{3/2}$ spectra and deconvoluted peaks attributable to Ni^{2+} and Ni^{3+} ions (b) the Mn $2p_{3/2}$ spectra and deconvoluted peaks attributable to Mn^{3+} and Mn^{4+} ions.

of different elements in $LiNi_{0.5}Mn_{1.5}O_4$. The Ni $2p_{3/2}$ XPS spectra of pristine $LiNi_{0.5}Mn_{1.5}O_4$ and surface-treated one are shown in Fig. 2(a). The Ni $2p_{3/2}$ binding energy of pristine $LiNi_{0.5}Mn_{1.5}O_4$ is located at ~854.8 eV, whereas that of surface-treated one using nitric acid is increased to ~855.1 eV. Considering that Ni^{3+} and Ni^{2+} each give rise to the Ni $2p_{3/2}$ binding energies at 855.8 and 854.5 eV, this positive shift seems to originate from the partial oxidation from Ni^{2+} to Ni^{3+} [18,19]. Because both pristine $LiNi_{0.5}Mn_{1.5}O_4$ and surface-treated one are primarily engaged in *Fd3m*, in which Ni and Mn ions are all located in 16d octahedral sites, the oxidation of Ni ions naturally breaks the electrostatic charge balance. Fig. 2(b) explains how the charge balance is reconstructed in surface-treated $LiNi_{0.5}Mn_{1.5}O_4$. Its Mn $2p_{3/2}$ binding energy is negatively shifted to ~642.3 eV indicating that Mn ions in 16d octahedral sites are partially reduced to Mn^{3+} (The Mn $2p_{3/2}$ XPS binding energies of Mn^{3+} and Mn^{4+} are 641.9 and 643.2 eV, respectively.) [20,21]. The atomic concentrations of the tested samples, obtained using the Mn $2p_{3/2}$ and Ni $2p_{3/2}$ spectra, indicated clearly that the partial reduction of Mn as well as the partial oxidation of Ni was induced by the nitric acid treatment (Table 1). From the depth profiles of the Ni and Mn atoms, shown in Fig. 3, it was apparent that the partial changes in the oxidation states of the Ni and Mn atoms were confined to the surface of the $LiNi_{0.5}Mn_{1.5}O_4$ sample. This phenomenon confirmed that, as a result of the nitric acid treatment, the 16d octahedral sites on the surfaces of the $LiNi_{0.5}Mn_{1.5}O_4$ particles exhibited a more disordered arrangement of the transition metals. This was owing to the transfer of electrons from Ni to the other transition metals, a phenomenon that has been reported to reduce the degree of cation ordering in Ni-containing compounds [20,22]. As shown in Fig. S3, there were no morphological changes in the treated sample after the nitric acid treatment, even though this treatment resulted in the partial reduction of Mn atoms, along with the partial oxidation of Ni atoms. Results of a Brunauer–Emmett–Teller (BET) analysis, shown in Table S1, also suggested that the change induced by the nitric acid treatment on the surface of the $LiNi_{0.5}Mn_{1.5}O_4$ sample was very small. This small change was attributed to the destruction of the surface oxidation layer by the nitric acid treatment, as proven by the elemental depth profiles of the pristine $LiNi_{0.5}Mn_{1.5}O_4$ and surface-treated $LiNi_{0.5}Mn_{1.5}O_4$ samples, shown in Fig. S4.

The Raman spectra of $LiNi_{0.5}Mn_{1.5}O_4$ before or after nitric acid treatment are given in Fig. 4. According to Oh et al., the strong band around 635 cm^{-1} is assigned to the symmetric Mn–O stretching mode of MnO_6 octahedra, whereas both peaks around 402 and 491 cm^{-1} are associated with the Ni^{2+}–O stretching mode. Another peak near 580–608 cm^{-1} is considered as $T_{2g}^{(3)}$ of the spinel compound whose splitting is obviously indicative of the ordered structure engaged in $P4_332$. The strong bands around 400, 239, 218 and 161 cm^{-1} are also attributed to $P4_332$. In addition, all reflections from $P4_332$ spinel tend to be sharper and better resolved than *Fd3m* spinel [23]. Fig. 4 shows that the $T_{2g}^{(3)}$ band for pristine $LiNi_{0.5}Mn_{1.5}O_4$ is clearly split between 606 and 589 cm^{-1}, and two broad humps appear around 239 and 218 cm^{-1}. In case of the conventional $LiNi_{0.5}Mn_{1.5}O_4$ with perfect primitive simple cubic structure ($P4_332$), the peak intensity at 161 cm^{-1} is much higher than the other two major peaks in 491 cm^{-1} and 635 cm^{-1}. Hence, the relatively reduced peak at 161 cm^{-1} for pristine $LiNi_{0.5}Mn_{1.5}O_4$

Table 1
The atomic concentrations determined by the fitting Mn $2p_{3/2}$ and Ni $2p_{3/2}$ spectra via Gaussian–Lorentz curve fitting.

Sample	Mn $2p_{3/2}$ atomic concentration %		Ni $2p_{3/2}$ atomic concentration %	
	Mn^{3+}	Mn^{4+}	Ni^{2+}	Ni^{3+}
Pristine $LiNi_{0.5}Mn_{1.5}O_4$	35.0	65.0	30.3	69.6
Treated $LiNi_{0.5}Mn_{1.5}O_4$	39.6	60.4	24.5	75.5

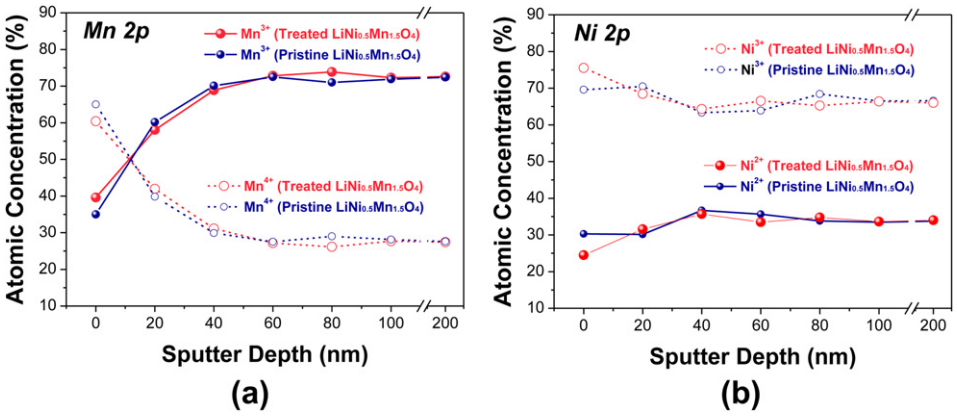

Fig. 3. Changes in the depth profiles of Ni and M ions in $LiNi_{0.5}Mn_{1.5}O_4$ after the nitric acid treatment.

points out that its structure is constructed by the mixed framework comprised of not only *P4₃32* but also *Fd3m* in accordance with XRD refinement analysis [24]. Nitric acid treatment significantly reduces the intensities of peaks at 635, 491 and 161 cm^{-1} as shown in Fig. 4. It means that its surface structure becomes more *Fd3m*-like together with the weakening of Mn–O bonds and Ni–O bonds followed by the reduced cation ordering in 16d octahedral site (Fig. 5).

The cyclic voltammetry (CV) curves of pristine $LiNi_{0.5}Mn_{1.5}O_4$ and surface-treated $LiNi_{0.5}Mn_{1.5}O_4$ using nitric acid are shown in Fig. S5. The double peak profile in the range of 4.4–4.6 V during reduction can be assigned to the two-step oxidation of Ni^{2+} to Ni^{3+}, and Ni^{3+} to Ni^{4+} [25]. Particularly, the intensity of peak attributed to the Ni^{2+}/Ni^{3+} redox couple is reduced by nitric acid treatment, while a small redox peak in 4 V region is more developed indicating that Mn^{3+}/Mn^{4+} redox reaction is activated as a result of nitric acid treatment. It resultantly indicates that the oxidation of Ni^{2+} to Ni^{3+} induce the reduction of Mn^{4+} to Mn^{3+} for the electrostatic charge balance, as confirmed by XPS. Fig. 6(a) compares the charge/discharge profiles of pristine $LiNi_{0.5}Mn_{1.5}O_4$ and surface-treated $LiNi_{0.5}Mn_{1.5}O_4$ using nitric acid during cycling. For all samples, two distinct plateaus are observed around 4.7 V, which arise from the consecutive reduction from Ni^{2+} to Ni^{4+}, and there is a small plateau in 4 V region linked to Mn^{3+}/Mn^{4+} [10,11]. Even if the CV curve of surface-treated $LiNi_{0.5}Mn_{1.5}O_4$ looks almost void of the trace of Ni^{2+}, this observation shows that the effect of nitric acid treatment is just confined to the surface of pristine sample. However, the larger capacity in the 4 V region of surface-treated sample compared to pristine sample is apparently evident of the increased amount of Mn^{3+} by nitric acid treatment in good agreement with XPS and CV analyses. Because the plateau around 4 V is regarded as a clear evidence of *Fd3m* disordered structure where the 16d octahedral sites have a disordered array of cations, the electrochemical properties of $LiNi_{0.5}Mn_{1.5}O_4$ is inevitably influenced by this treatment. Compared to *Fd3m* disordered structure having one-step phase transition between two cubic phases, *P4₃32* ordered structure would get much larger strain during lithiation/delithiation, originating from two-step phase transitions between three cubic phases [26]. The extended cycling to 100th cycle at 55 °C makes pristine $LiNi_{0.5}Mn_{1.5}O_4$ (Fig. 6(a)) suffer from significant polarization increase followed by severe capacity fading. Contrarily, the polarization change of surface-treated

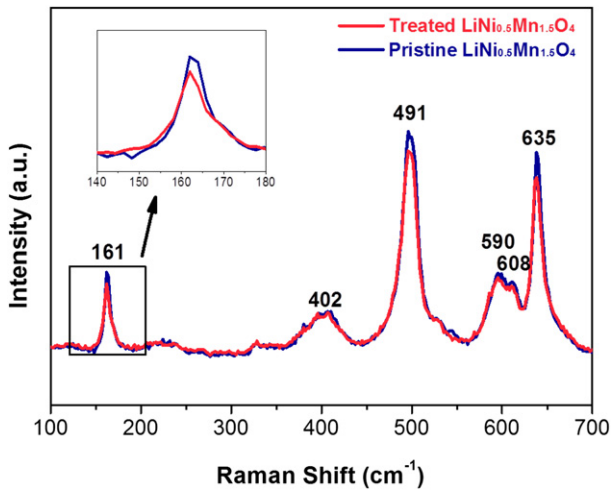

Fig. 4. Raman spectra of the pristine $LiNi_{0.5}Mn_{1.5}O_4$ and surface-treated $LiNi_{0.5}Mn_{1.5}O_4$ samples.

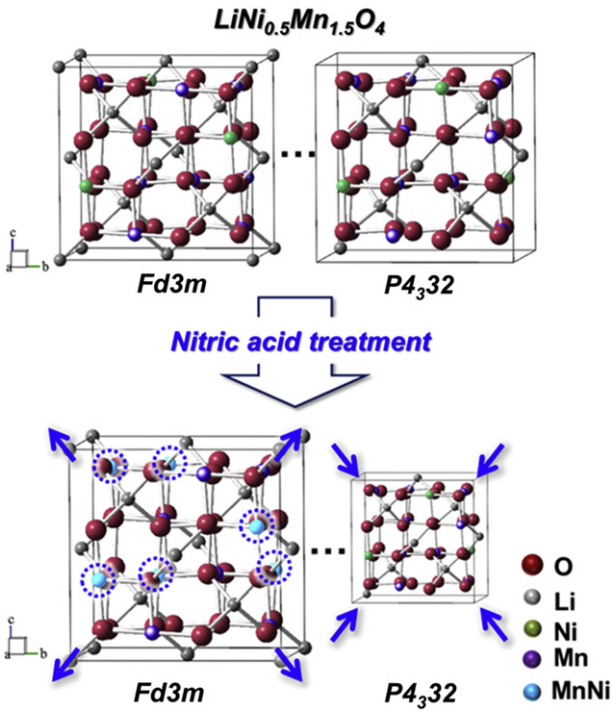

Fig. 5. Schematic illustration of the structural changes induced in $LiNi_{0.5}Mn_{1.5}O_4$ by the nitric acid treatment.

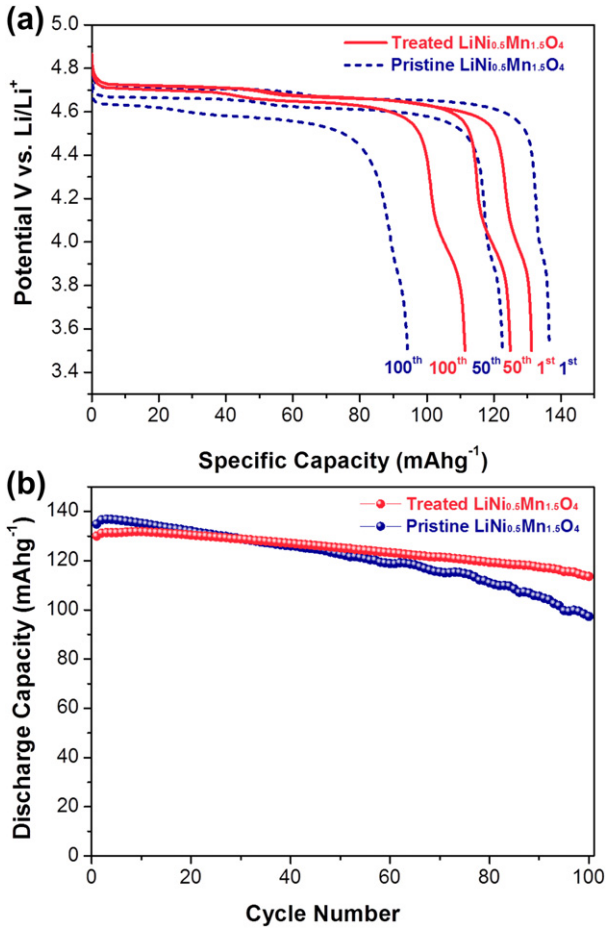

Fig. 6. (a) Charge/discharge curves of the pristine $LiNi_{0.5}Mn_{1.5}O_4$ and surface-treated $LiNi_{0.5}Mn_{1.5}O_4$ samples after the 1st, 50th, and 100th cycle at 55 °C. (b) Electrochemical cycling performances of the pristine $LiNi_{0.5}Mn_{1.5}O_4$ and surface-treated $LiNi_{0.5}Mn_{1.5}O_4$ samples.

$LiNi_{0.5}Mn_{1.5}O_4$ is relatively insignificant achieving an excellent cyclic stability. Fig. 6(b) shows that nitric acid treatment greatly enhances the cyclic stability of pristine $LiNi_{0.5}Mn_{1.5}O_4$. Actually, its cyclic retention has been improved from 72% of the initial capacity to 87% after 100 cycles at 55 °C, respectively. The electrochemical superiority of surface-treated $LiNi_{0.5}Mn_{1.5}O_4$ is believed to result from the reduced cation ordering induced by the partial reduction of Mn ions. Previous studies have shown that the electrochemical superiority of the *Fd3m* space group to the $P4_332$ group is associated with higher electronic conductivity, lower degree of polarization, and lower activation energy [27]. Because the surface-treated $LiNi_{0.5}Mn_{1.5}O_4$ sample had a surface structure that was more *Fd3m*-like, as had been indicated by the results of the various analyses, the nitric acid treatment had a positive effect on the electrochemical properties of $LiNi_{0.5}Mn_{1.5}O_4$. The slight reduction in polarization seen in the cyclic voltammetry curve of the surface-treated $LiNi_{0.5}Mn_{1.5}O_4$ sample was also evidence of this positive effect (Fig. S5). In addition, even though Mn^{3+} ions have generally been reported to have negative effects on $LiMn_2O_4$, owing to the Jahn–Teller distortion and the dissolution of Mn, a number of research groups have already demonstrated that the disordered structure (*Fd3m*) induced primarily by the Mn^{3+} ions tends to improve the electrochemical performance of $LiNi_{0.5}Mn_{1.5}O_4$ [24,26,28,29]. However, the correlation between the concentration of Mn^{3+} ions in $LiNi_{0.5}Mn_{1.5}O_4$ and their effect on its electrochemical performance need to be elucidated further. In this study, the elemental depth profile of the surface-treated $LiNi_{0.5}Mn_{1.5}O_4$ sample provided significant clues about this phenomenon. Fig. S4 shows that the surface concentration of Mn was lower compared to that of the bulk, reducing the possibility of Mn dissolution at high temperatures. As for the Jahn–Teller distortion, the disordered 16d sites composed of Mn and Ni atoms seem to be the key against the electrochemical degradation induced by the distortion.

4. Conclusion

In summary, we have demonstrated that reducing the degree of cation ordering in the 16d octahedral site of $LiNi_{0.5}Mn_{1.5}O_4$ is an effective way to improve its electrochemical properties especially at high temperature. XRD patterns coupled with XPS and Raman spectra indicate that nitric acid treatment renders pristine $LiNi_{0.5}Mn_{1.5}O_4$ more *Fd3m*-like together with the reduced cation ordering in 16d octahedral site. Thanks to this characteristic structural change, surface-treated $LiNi_{0.5}Mn_{1.5}O_4$ using nitric acid shows a superb cyclic stability that 87% of the initial capacity is still maintained after 100th charge/discharge.

Acknowledgment

This research was supported by the Converging Research Center Program through the Ministry of Education, Science and Technology (2012K001257).

Appendix A. Supplementary data

Supplementary data related to this article can be found at http://dx.doi.org/10.1016/j.jpowsour.2012.12.051.

References

[1] Y. Nishi, J. Power Sources 100 (2001) 101.
[2] S. Megahed, B. Scrosati, J. Power Sources 51 (1994) 79.
[3] J.M. Tarascon, B. Guyomard, J. Electrochem. Soc. 138 (1991) 2864.
[4] S.H. Park, K.S. Park, Y.K. Sun, K.S. Nahm, J. Electrochem. Soc. 147 (2000) 2116.
[5] R.J. Gummow, A. de Kock, M.M. Thackeray, Solid State Ionics 69 (1994) 59.
[6] M.M. Thackeray, Y. Shao-Horn, A.J. Kahaian, Electrochem. Solid-State Lett. 1 (1998) 7.
[7] D.H. Jang, Y.J. Shin, S.M. Oh, J. Electrochem. Soc. 143 (1996) 2204.
[8] Y. Xia, Y. Zhou, M. Yoshio, J. Electrochem. Soc. 144 (1997) 2593.
[9] P. Arora, B.N. Popov, R.E. White, J. Electrochem. Soc. 145 (1998) 807.
[10] K. Amine, H. Tukamoto, H. Yasuda, Y. Fujita, J. Electrochem. Soc. 143 (1996) 1607.
[11] Q. Zhong, A. Bonakdarpour, M. Zhang, Y. Gao, J.R. Dahn, J. Electrochem. Soc. 144 (1997) 205.
[12] T. Ohzuku, S. Takeda, M. Iwanaga, J. Power Sources 81 (1999) 90.
[13] R. Santhanam, B. Rambabu, J. Power Sources 195 (2010) 5442.
[14] T. Noguchi, I. Yamazaki, T. Numata, M. Shirakata, J. Power Sources 174 (2007) 359.
[15] Y.S. Lee, Y.M. Todorov, T. Konishi, M. Yoshio, ITE Lett. 1 (2001) 1.
[16] P. Strobel, A. Ibarra Palos, M. Anne, F. Le Cras, J. Mater. Chem. 10 (2000) 429.
[17] K. Ariyoshi, Y. Iwakoshi, N. Nakayama, T. Ohzuku, J. Electrochem. Soc. 151 (2004) A296.
[18] K.S. Kim, N. Winograd, Surf. Sci. 43 (1974) 625.
[19] K. Amine, H. Tukamoto, H. Yasuda, Y. Fujita, J. Power Sources 68 (1997) 604.
[20] K.M. Shaju, G.V. Subba Rao, B.V.R. Chowdari, Solid State Ionics 152–153 (2002) 69.
[21] W. Branford, M.A. Green, Chem. Mater. 14 (2002) 1649.
[22] S.H. Oh, K.Y. Chung, S.H. Jeon, C.S. Kim, W.I. Cho, B.W. Cho, J. Alloys Compd. 469 (2009) 244.
[23] G.B. Zhong, Y.Y. Wang, Y.Q. Yu, C.H. Chen, J. Power Sources 205 (2012) 385.
[24] M. Kunduraciz, G.G. Amatucci, J. Electrochem. Soc. 153 (2006) A1345.
[25] G.T.K. Fey, C.Z. Lu, T.P. Kumar, J. Power Sources 115 (2003) 332.
[26] J.-H. Kim, S.-T. Myung, C.S. Yoon, S.G. Kang, Y.-K. Sun, Chem. Mater. 16 (2004) 906.
[27] L. Wang, H. Li, X. Huang, E. Baudrin, Solid State Ionics 193 (2011) 32.
[28] J. Cabana, M.C. Cabanas, F.O. Omenya, N.A. Chernova, D. Zeng, M.S. Whittingham, C.P. Grey, Chem. Mater. 24 (2012) 2952.
[29] J. Xiao, X. Chen, P.V. Sushko, M.L. Sushko, L. Kovarik, J. Feng, Z. Deng, J. Zheng, G.L. Graff, Z. Nie, D. Choi, J. Liu, J.-G. Zhang, M.S. Whittingham, Adv. Mater. 24 (2012) 2109.